



---

**Bisphenol A Detection on a Carbon Graphite Electrode  
Modified with a Polyaniline- 2,2'-Azinobis-(3-Ethyl  
Benzothiazolin-6-Sulfonic Acid) Composite using  
Horseradish Peroxidase Enzyme as a Bio-recognition Unit,  
Preliminary Results**

Linet Ogallo<sup>a</sup>, Immaculate N. Michira<sup>b\*</sup>, Damaris N. Mbui<sup>c</sup>

<sup>a,b,c</sup>Chemistry department university of Nairobi, 30197, Nairobi, 00100, Kenya

<sup>a</sup>Email: [ogalolyn@students.uonbi.ac.ke](mailto:ogalolyn@students.uonbi.ac.ke), <sup>b</sup>Email: [imichira@uonbi.ac.ke](mailto:imichira@uonbi.ac.ke)

<sup>c</sup>Email: [dmbui@uonbi.ac.ke](mailto:dmbui@uonbi.ac.ke)

**Abstract**

Bisphenol A is an endocrine disruptor which is almost ubiquitous. It is found in plastics, supermarket thermal receipts, CDs, food containers, water bottles, building materials amongst others. Bisphenol A has been associated with serious health issues ranging from obesity to cancer. This study aimed at developing an electrochemical method for the detection of bisphenol A in the environment. Horse radish peroxidase enzyme encapsulated on a modified polyaniline graphite carbon paste electrode was the recognition system. All electrochemical experiments were done on the cyclic voltammetric mode. The conducting properties of the polyaniline- Polyaniline 2, 2'-Azinobis [3-ethylbenzothiazoline-6-sulfonic acid] polymer composites were carried out using UV-Vis spectrophotometry. The presence of polaron and bipolaron bands in the UV-Vis spectra at around 446 nm and or greater than 650 nm indicated improved polymer conductivity. Preliminary results for the HRP/H<sub>2</sub>O<sub>2</sub> system displayed a  $1.54 \times 10^{-4}$  peak current signal de-attenuation on addition of cumulative aliquots of 0 – 2500 nM. The greater than 90% signal de-attenuation was due to presence of BPA provided- a basis for creating a BPA detection methodology based on inhibition in future studies.

**Keywords:** Bisphenol A Biosensor; Composite; Carbon Graphite Electrode; ABTS doped polyaniline.

---

\* Corresponding author.

## **1. Introduction**

Bisphenol A is a monomer used to produce polycarbonate plastics (PC), a major precursor in resin lining manufacturing for food cans, aluminium water bottles amongst others. The annual BPA global production capacity exceeds 6.4 billion pounds [1]. The consumption by volume globally of BPA, for different applications, was about 7.7 million metric tonnes by 2015. This increased to 8 million metric tonnes in 2016 and with an estimated compound annual growth rate (CAGR) of 4.8 % is projected to be 10.6 million metric tonnes by 2022. The demand of the compound globally is expected to rise to 5.4% over this period and the expenditure estimated to rise to USD 22.5 billion in 2022 from 16.4 billion in 2016. The largest market for BPA is Asia (Pacific) which is 53% of the total share with 36% going to USA and Europe [2]. This is an indication that there is increase in consumption of BPA despite its prohibited use in baby bottles in Europe, USA and Canada.

Bisphenol A is used to harden plastics, making the transparent and colourful Nalgene-type water bottles shatter-proof and unbreakable [3]. Plastics have a recycle code at the bottom ranging from 1 to 8 encoded in a triangle with racing arrows. Those with recycle number 7 labelled as HPDE 7 are polycarbonates (PC) and may contain Bisphenol A (BPA) as an additive. The polycarbonate (PC) plastic is resistant, rigid and transparent thermoplastic. Some of these properties conferred by bisphenol A [4] makes it more preferred for use in liquid and food containers such as cups, baby feeding bottles and water tanks. Furthermore, the plastic is also used in lining/making residential water storage containers [5]. BPA is also used in the manufacture of carbonless copy paper, sports equipment, medical dental devices, dental fillings and sealants, eyeglass lenses, CDs and DVDs, household electronics.

However, bisphenol A (BPA) is considered an environmental oestrogen. Migration of BPA from these contact materials to food has been discussed [6]. In many developed countries, the use of BPA in the manufacture of plastics especially on baby bottles has been banned [7]. This is due to the health concerns associated with its use. Dangers associated with BPA exposure include, early maturity especially among girls, sexual dysfunction, neurological disorders, asthma, thyroid dysfunction, breast and prostate cancer. Others include obesity, DNA methylation and disruption of the dopaminergic system oxidative stress and repeated miscarriages [8, 9].

In developing countries, the use of such PC plastics continues, a situation that exposes millions of human beings to such untold health risks because there is a possibility that the concentration of leachate BPA is well above the allowable limit. The fact that polycarbonate-based containers are still in use in Kenya/developing countries could be due to lack of affordable alternatives or simply a lack of awareness as to the dangers of using BPA polycarbonate plastics.

Analysis of Bisphenol A using various techniques such as gas chromatography, nuclear magnetic resonance (NMR) has been found to be expensive, require skilled labour and is limited to centralized laboratories therefore it is not easy to monitor the levels of BPA in the environment, especially in a developing country like Kenya. Since BPA is an electroactive compound that gives rise to a well-defined redox couple, it is envisaged that by coupling the redox activity of BPA to that of a suitable oxido-reductase enzyme, an alternative electrochemical based methodology for the detection of the BPA toxin can be developed.

This work therefore, proposes the fabrication of a polyaniline 2, 2'-Azinobis [3-ethylbenzothiazoline-6-sulfonic acid] (ABTS) composite and its use in modification of a polished spent dry-cell graphite electrode. The encapsulation of a horseradish peroxidase enzyme onto the polyaniline- 2, 2'-Azinobis [3-ethylbenzothiazoline-6-sulfonic acid] (ABTS) composite modified graphite electrode will yield a sensor for BPA. The horseradish peroxidase (HRP) enzyme bio-recognition unit was chosen due to its affordability, stability and easy storage coupled with the fact that it catalyses the breakdown of phenols. HRP is a choice enzyme in most biosensor systems because one of its substrate hydrogen peroxide- a major by-product of many biological catalytic activities [10].

## **2. Methods and materials**

### **2.1. Experimental reagents**

All the chemicals used in this work were of analytical grade unless otherwise stated. Horseradish peroxidase (E.C 1.11.1.7) 100 mg (Sigma), aniline (99% w, v) and hydrochloric acid (37% w, v) methanol (Fluka manufacturers), Anhydrous disodium hydrogen phosphate and Anhydrous potassium dihydrogen phosphate were bought locally. Methanol (99% purity, from Fluka, bisphenol A standard (99% purity, Sigma-Aldrich), 2, 2'-Azinobis (3-ethylbenzothiazoline-6-sulfonic acid) (ABTS), Potassium per sulphate 98%, dimethyl sulfoxide (DMSO), 30% by volume hydrogen peroxide were purchased locally.

### **2.2. Electrode preparation**

#### **2.2.1. Preparation of working electrode**

The carbon graphite rods were extracted from spent dry cell battery, washed and rinsed thoroughly with distilled water before being left to dry for a week. Then using sand paper numbers 400, 500 and 600 respectively, the dry graphite rods were polished. Finally, on rubbing the sand paper polished surfaces onto a thoroughly cleaned glass under running tap water for 5 minutes, a shiny mirror-like surface was obtained. The electrode was designated as, graphite carbon electrode (GCE).

The potentiostatic calibrations were performed using the as-prepared shiny mirror like GCE electrodes and potassium ferricyanide solutions on the using cyclic voltammetry mode. Calibration was done by running cyclic voltammograms (CVs) of 25 mL solutions of potassium ferricyanide in the concentration ranges 0.01 to 0.1 M. Scanning was done in 0.1 M KNO<sub>3</sub> as supporting electrolyte at different scan rates and then examining the difference in the anodic/cathodic ( $\Delta E_p$ ) peak potentials of the redox couple. A platinum counter electrode and a saturated calomel electrode (SCE) reference electrode were used.

Electrode hygiene after each scan was maintained by repeating the polishing process as described above. The platinum wire auxiliary electrode was thoroughly cleaned with distilled water and the tip then passed through a non-luminous flame to remove all adsorbed impurities.

#### **2.3. Electrosynthesis of polyaniline/2, 2'-Azinobis [3-ethylbenzothiazoline-6-sulfonic acid] (ABTS) film**

### ***2.3.1. Preparation of electrolyte and monomer solutions***

A 100ml stock solution of 1M of HCl was prepared. From which batch concentrations of 0.1 and 0.5 M HCl acid were prepared by serial dilution. HCl was employed as the supporting electrolyte during the oxidative polymerization of aniline in the presence and /or absence of the 2, 2'-Azinobis [3-ethylbenzothiazoline-6-sulfonic acid] (ABTS) stabilizing surfactant.

Polyaniline films were cast from either 0.1 or 1 M aniline solutions in 25 mL of the already prepared 1M HCl stock solution. Prior to any synthesis, the aniline monomer was purified by fractional distillation to a clear liquid collected between 175-177 °C and consequently stored in brown bottles to avoid re-oxidation that occurs when exposed to light.

Electrochemical synthesis was carried out at room temperature using the mirror polished spent battery graphite carbon electrode (GCE) as the working electrode with an active area diameter of 0.64 cm<sup>2</sup>. The counter and the reference electrodes were as stated above. The bioanalytical systems potentiostat (BAS) was operated on the cyclic voltammetric mode and operated between switch potentials -0.1 to 1 V at a scan rate of 10 and 20 mV/s. Potential cycling was done for 5 and 10 cycles respectively.

### ***2.4. Chemical synthesis of polyaniline/ABTS composites***

The chemical synthesis of polyaniline and/or polyaniline ABTS was done using potassium persulphate (K<sub>2</sub>S<sub>2</sub>O<sub>8</sub>) as the oxidant in the presence or absence of HCl.

A 1:1:1 acid to monomer to oxidant mole ratio was prepared as follows. Into a solution containing 2.1 mL of 37% (w,v) hydrochloric acid in distilled water, 2.3 mL of aniline with stirring to complete dissolution in a 25mL volumetric flask. The volume was then topped up to the mark. Separately, 0.847g of potassium per sulphate was dissolved in distilled water in a 25 ml volumetric flask and then topped to the mark. The solutions were cooled in an ice bath for 15 minutes and then mixed together. The reaction was allowed to continue in the ice bath with concurrent magnetic stirring for two hours. The solid mixture formed was left to cool for 30 minutes and the green precipitate formed was filtered off, doubly washed with distilled water before being oven dried at 60<sup>0</sup> C for 48 hours. Later, the green cake was pulverised using a mortar and pestle and stored in dark brown vials for future use. The procedure was repeated in the absence of the oxidant.

### ***2.5. Characterisation of the Electrosynthesized and Chemically synthesized Polymer composites***

All electrochemical measurements were done on a Bioanalytical Systems (BAS) potentiostat interfaced with a Pentium 3 intel computer for all data recording/processing. The potentiostat was operated mainly on the cyclic voltammetric mode with potential been cycled at different scan rates. For all experiments, HCl was the supporting electrolyte.

### ***2.6. Spectrophotometric characterization of the Polymer Composites***

### **2.6.1. UV-Vis spectroscopy**

The conductive nature of the PANI and modified PANI films was also determined using UV-Vis spectroscopy. Scanning was done in DMSO solvent on a Ultrospect 3 LKB spectrophotometer. UV-Vis spectra for the electrosynthesized films were obtained by dipping the films in 1 mL DMSO to yield green solutions that were subjected to UV-Vis scanning. For the chemically as-synthesized films, 0.2 g quantity of the green powders were dispersed in 10 mL DMSO before being poured into 1 mL glass cuvettes. For all the solutions scanning was done between 350nm and 700nm. De-doping was done by adding 5 mL of 0.5 M ammonia solution into the DMSO solutions where necessary.

### **2.7. Preparation of buffer solution pH 7 as working solutions for the biosensor**

Separately, 250 mL each of 0.1 M potassium dihydrogen phosphate and 0.25 M disodium hydrogen phosphate were prepared. Precisely, 3.4025 g of  $\text{KH}_2\text{PO}_4$  was dissolved in a little distilled water in a beaker stirred, transferred into a 250ml volumetric flask. Exactly, 1.8637 g of Potassium chloride (0.1 M KCl) was added to the same flask with shaking unto complete dissolution upon which distilled water was added to the mark. Separately, a 0.25 M disodium hydrogen phosphate  $\text{Na}_2\text{HPO}_4$  was constituted by dissolving 8.750g of the salt in a little distilled water in a 250 mL flask and topping up to the mark.

100 mL of 0.1 M potassium dihydrogen phosphate  $\text{KH}_2\text{PO}_4$  solution prepared above recorded a pH of about 4. By adding aliquots of 0.25 M disodium hydrogen slowly under magnetic stirring a required phosphate buffer of pH 7 was constituted.

### **2.8. Encapsulation of the HRP enzyme**

Electrochemical characterization of the polymeric biosensors was done after encapsulating HRP within the polymeric matrices. About 10 mL of horseradish peroxidase (EC.1.11.1.7) solution (already constituted in phosphate buffer) was placed in a 25 mL volumetric flask and topped up to the mark using the 0.1 M phosphate buffer pH 7 prepared above. About 10  $\mu\text{L}$  of the resultant peroxidase solution was drop-coated onto the working electrode surface (CGE/PANI/ABTS), left to dry for 15 minutes under a fan, then further incubated in the refrigerator for 35 minutes. The enzyme electrodes were then rinsed carefully with 0.1 M phosphate buffer, pH 7.0 and stored under the same buffer in the refrigerator at 4  $^{\circ}\text{C}$  when not in use. The CGE/PANI/ABTS/HRP electrode constituted the enzyme modified working electrode.

### **2.9. Electrochemical Behaviour of the GCE/PANI-ABTS/HRP Electrode in 0.1 M Phosphate Buffer Solution in the presence/and or absence of hydrogen peroxide substrate**

The air dried GCE/PANI/ABTS/HRP was placed in a 25 mL 0.1 M phosphate solution and the potential cycled between -1.5 and 1.5 volts at different scan rates to scrutinize the electrochemical behaviour. A potential window of 0 to -1.250 V was eventually selected. A platinum counter electrode and SCE reference electrode was used. Prior to the addition of small aliquots the working electrode was lifted out of the buffer solution, thoroughly rinsed with distilled water and then placed in a fresh 25 mL 0.1 M phosphate to which small aliquots

of hydrogen peroxide were added. The potential was cycled at different scan rates and the resulting voltammograms were analysed.

### 2.10. Preparation of the BPA Standard Analyte Solution

A standard 100 mL stock solution of 0.025 mM BPA was prepared by dissolving 0.0057g of BPA in a little methanol and making it to 100 mL by methanol. Different volumes of BPA from this stock solution were used for biosensor response testing. BPA aliquots in the range 5- 1000 $\mu$ l were used.

The peroxidase- modified electrode was placed in a three-electrode cell with a standard calomel saturated KCl reference electrode and a platinum counter electrode in a 0.1 M phosphate buffer medium pH 7. The electrodes were fitted into the cell and connected to the PGSTAT 12 potentiostat and scanned from -0.1 to 1 V. Two drops of hydrogen peroxide were added into the buffer each time prior to the additions of different aliquots of 0.025 mM BPA.

## 3. Results

### 3.1. Potentiostat Calibration based on potassium ferricyanide redox response

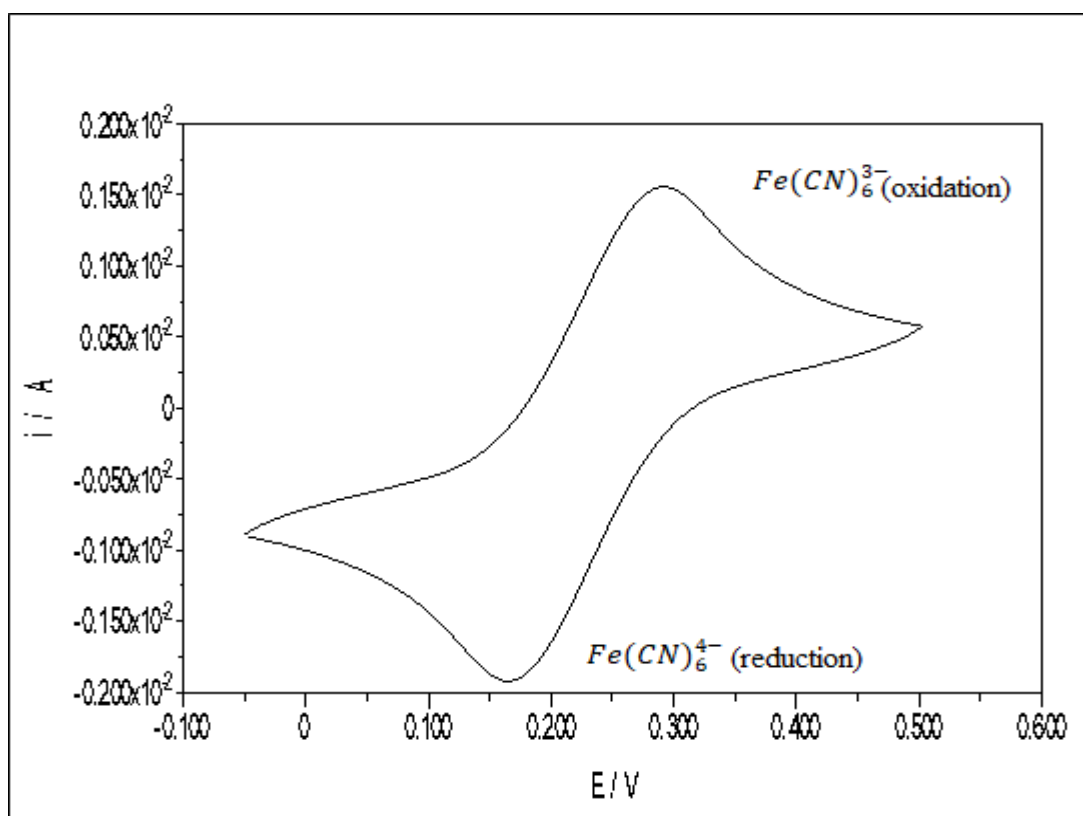


**Figure 1:** Cyclic voltammogram for 0.04 M ferricyanide standard showing a perfect  $Fe(CN)_6^{3-}/Fe(CN)_6^{4-}$  redox couple

All the cyclic voltammograms of the ferricyanide solutions despite the concentration displayed well formed redox peaks for the  $Fe(CN)_6^{3-}/Fe(CN)_6^{4-}$ . The redox reaction taking place can be represented by the equation;



Although the anodic to cathodic peak ratios ( $I_p_a/I_p_c$ ) for the redox couples were close to unity, the  $\Delta E_p$  values expected for a reversible system are  $59/n$  mV [11, 12]. The redox couple gave  $\Delta E_p$  greater than  $70/n$  mV indicating presence of other contributions e.g ohmic drop which could be rectified by placing the reference electrode very close to the working electrode. Figure 1 displays one of the ferricyanide voltammogram obtained.

### 3.2. Electrosynthesis of PANi/ABTS

Potential cycling on the Carbon graphite electrode, in an aniline/ABTS/HCl three electrode electrochemical bath produced green films adsorbed on to the CGE electrode surface corresponding to the polyemeraldine form of polyaniline. Three oxidation peaks were observed in the cyclic voltammograms (CVs), Fig. 2 and 3 below. The oxidation peaks observed at 0.19V, 0.45V, 0.85V and reduction counter waves at potentials of 0.03V, 0.43V and 0.68V belonged to the polyleucoemeraldine, polyemeraldine and polypernigraniline forms of PANi respectively.

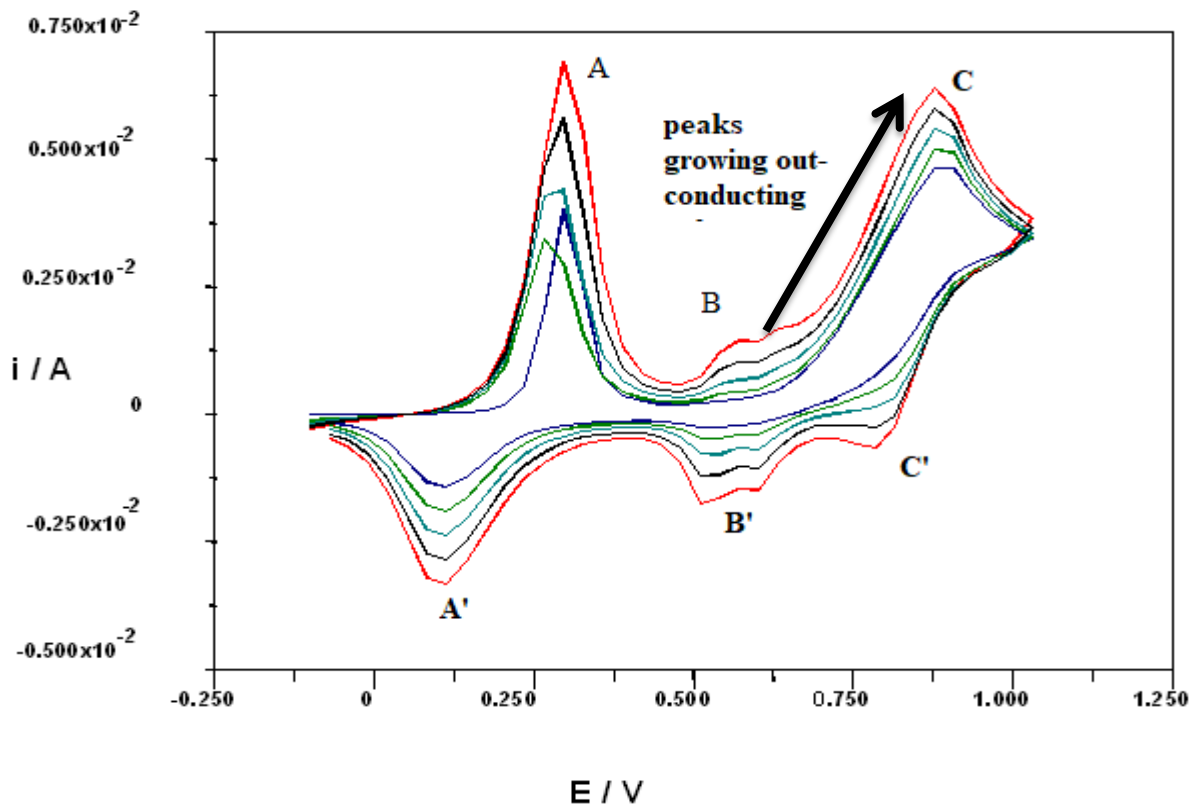


**Figure 2:** Cyclic voltammograms showing 5 Electrodeposition cycles of polyaniline/ABTS film at a scan rate of 50mV/s

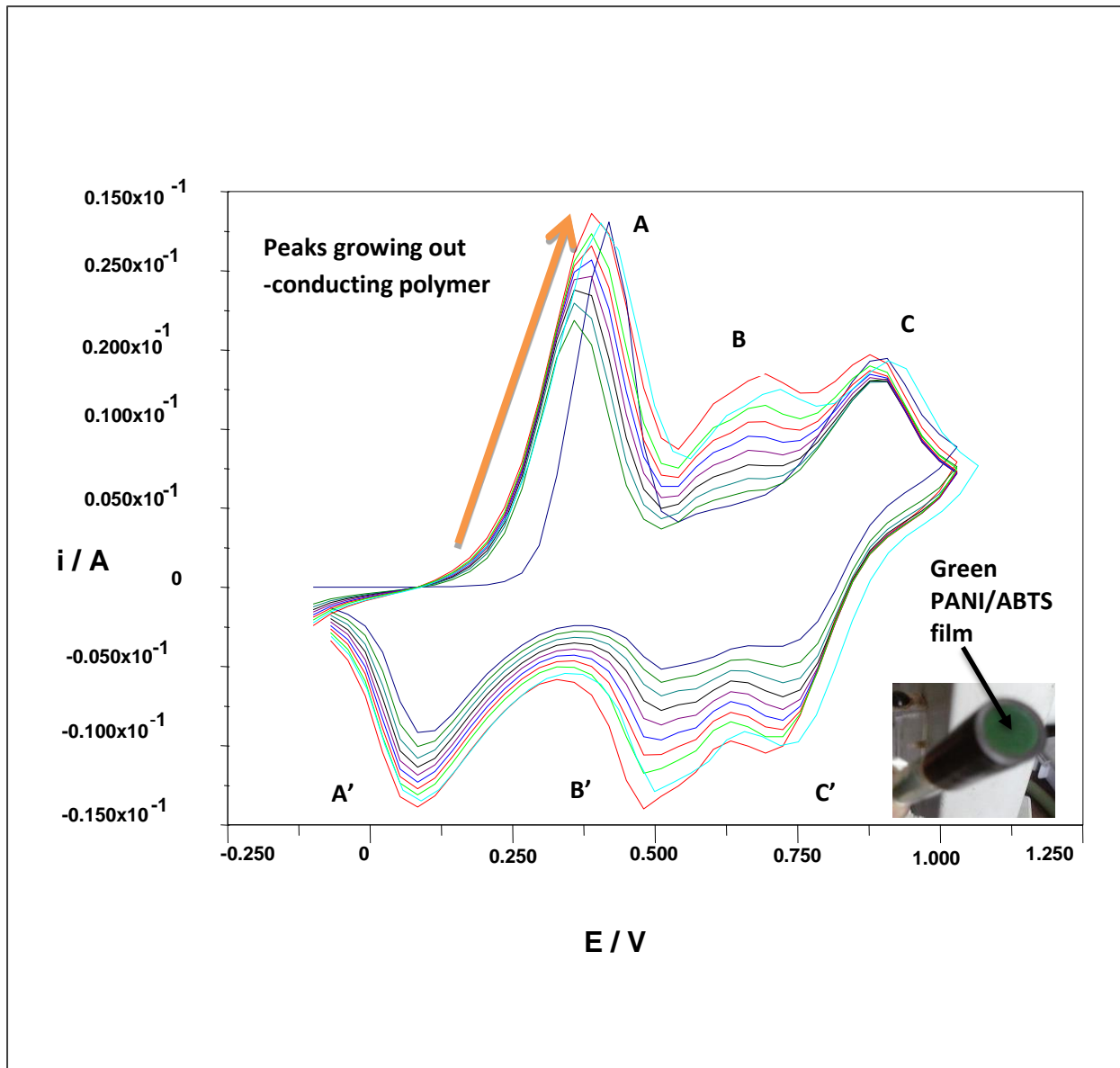


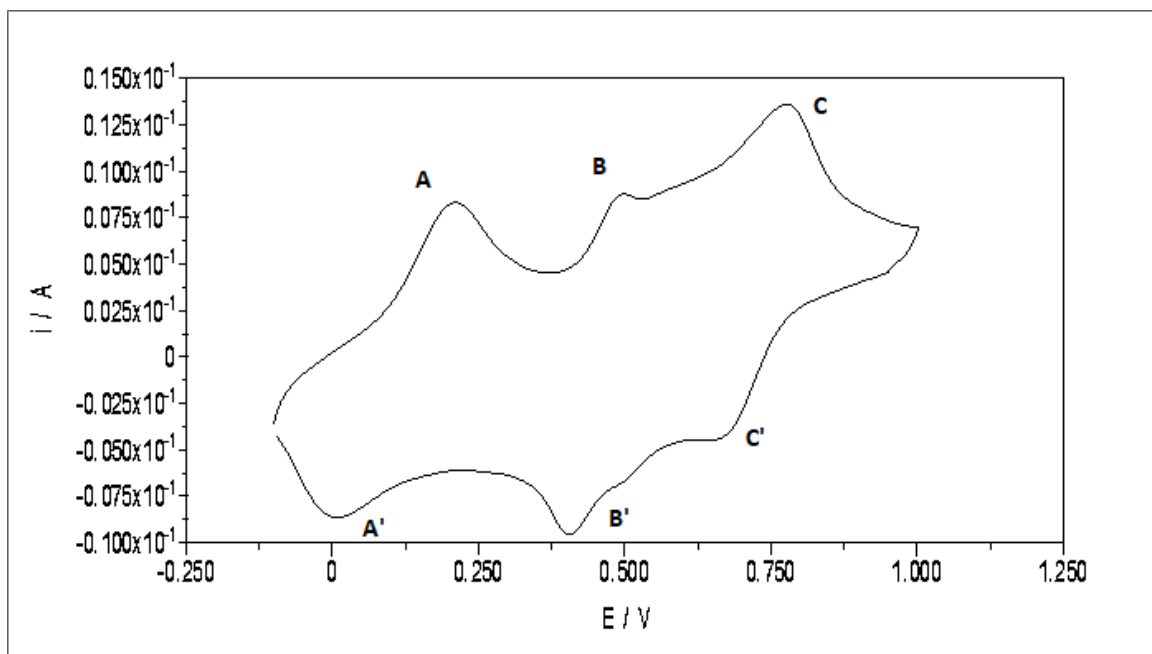
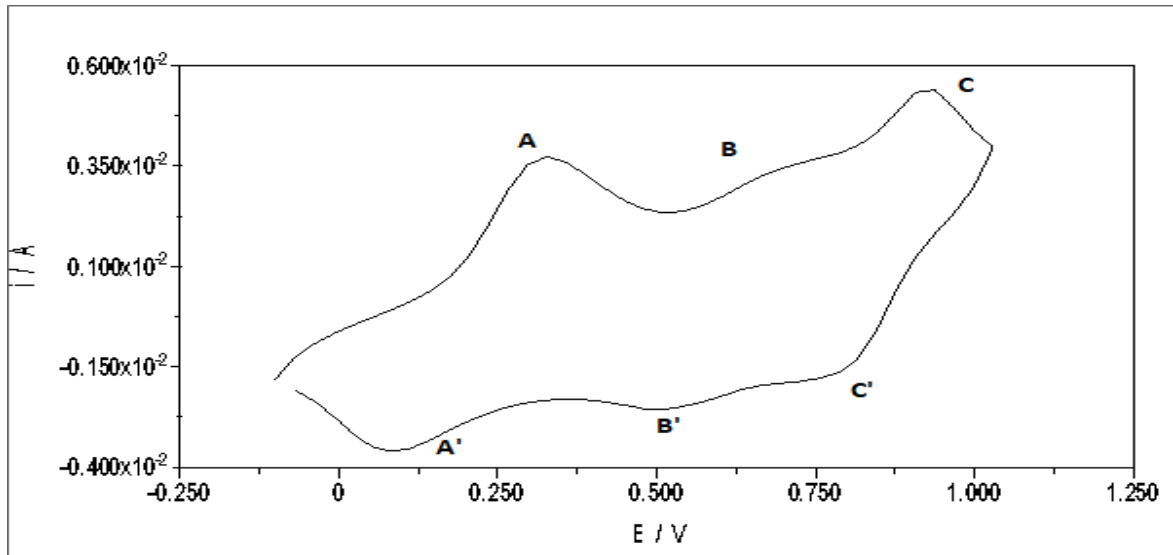
**Figure 3:** Cyclic Voltammograms for 10 electrodeposition cycles of Polyaniline /ABTS film at 100mV/s. Inset: The green electrodeposited peak of PANI/ABTS on the carbon graphite electrode (CGE)

The green polyemeraldine form of PANI is the most conductive. Generally, there are only three polyaniline allowed oxidation states, namely the fully reduced polyleucoemeraldine (PLE), the half oxidised polyemeraldine PEM and the fully-oxidised polypernigraniline (PPN) forms [13, 14]. Of the three forms it has reported that the polyemeraldine form (PEM) of PANi can easily undergo protonation leading to the formation of the polyemeraldine salt which is the most conductive form of PANi and which is green in colour, a phenomenon referred to as protonic doping [13-15].

### 3.3. Electrochemical Characterization of the PANi/ABTS cast thin films

The electrochemical characterization of the cast green PANi/ABTS films adsorbed onto the CGE electrode was carried out in dilute HCl which was the supporting electrolyte. The supporting electrolyte was helpful in

minimizing migration effects. Characterization was done to ensure the electroactivity of the films was maintained, a prerequisite for biosensor applications. A comparison of Figure 4 and 5 below shows the presence of ABTS enhances the electroactivity of the PANi films giving rise to well defined peaks an indicator of better electrochemistry.



**Figures 4 & 5:** Cyclic voltammograms of PANi/HCl and PANi/ABTS films at a scan rate of 100mV/s. Supporting electrolyte, 1M HCl. Concentration of ABTS,  $1 \times 10^{-4}$  M ABTS. Figure 5 shows better enhanced peaks in presence of surfactant

From the two voltammograms, it is clear that in the presence of the surfactant ABTS, both the oxidative and redox peaks are more pronounced than when in its absence. Even the conductivity of the film increased which

can be seen by the fact that the peak currents in the presence of the surfactant are a 10 magnitude higher. It has been argued the presence of a surfactant e.g ABTS can improve electrical sensitivity by accelerating the diffusion of the analyte/s to the electrode surface [16]. Similar results have been reported by [17], the presence of a surfactant during cyclic voltammetric characterization also improves the movement of flux so much so that even the limit of detection of the analyte is greatly lowered.

Table 1 below highlights the main differences between PANi-ABTS electrosynthetic film formed in the presence of surfactant (ABTS) and in its absence (i.e PANi/HCl). The Table gives the number of redox peaks in the synthesized polyaniline film, peak to peak separation ( $\Delta E$ , mV) and the magnitude of the current for the peaks ( $I_{\text{anodic}}$  and  $I_{\text{cathodic}}$ ).

**Table 1:** Comparison of redox activity for PANI/ABTS versus PANI/HCl

Film Type	PANI/ABTS	PANI/HCl
<b>Number of redox peaks</b>	3 sharp redox pairs	2 redox pairs that are not very pronounced
<b>Peak to peak separation (<math>\Delta E_p</math>, mV)</b>	Peak A/A' (125); peak B/B' (50), Peak C/C' (75)	Peak A/A (200);  Peak B/B' (not well formed)  Peak C/C' (187 mV)
<b>Current magnitude</b>	Peak A/A' (1.06)	Peak A/A' (0.7)
<b><math>I_{\text{pa}}/I_{\text{pc}}</math></b>	Peak (B/B') (0.92)	Peak B/B' (not well formed)  Peak C/C' (3)  Peak C/C' (2.6)

One of the common problems often experienced in carrying out cyclic voltammetry is the inability to duplicate the position of the electrode. Use of a Luggin capillary which was lacking could solve this. Another problem could be the occurrence of electrode side reactions. Despite all these, from the table, it is seen that the presence of a surfactant yields better electrochemistry than its absence given that the peak to peak separations are near Nernstian for reversible electrochemistry and the ratio of peak heights approaches one for the first two redox couples.

### 3.4. Peak current dependence of the PANi/ABTS film (Randles Sevcick plot)

As had been indicated earlier, better peak enhancement was observed at lower monomer concentrations and surfactant prepared films exhibited better electrochemistry. Thus the PANi/ABTS system at low scan rates was

subjected to Randles Sevcick analysis. The PANi/ABTS film was cast on a carbon graphite electrode (CGE) and the potential cycling of the film done at different scan rates. The resultant voltammograms were presented as distinct voltammograms (figure 6) since overlaying of the voltammograms was not supported by the equipment.

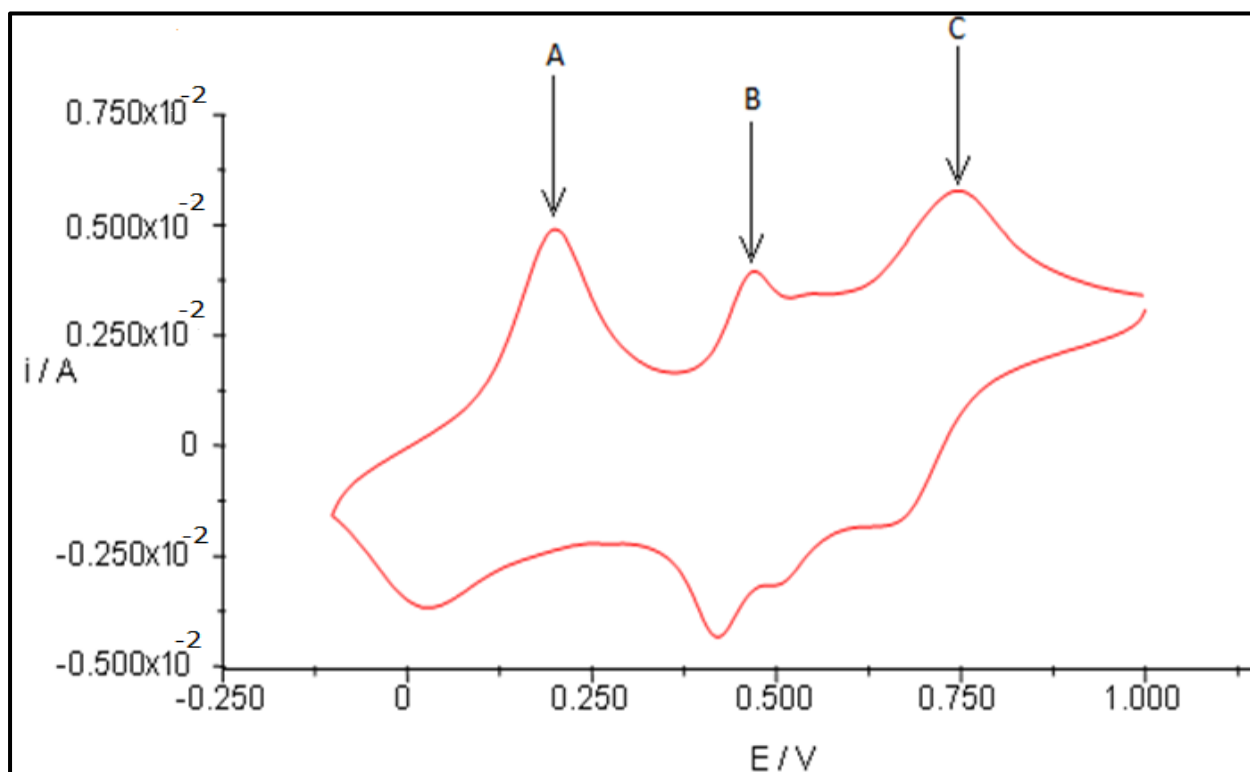


**Figure 6:** CV of PANI ABTS at low scan rate. Low scan rate allow time for diffusion of flux leading to better electrochemistry

Analysis of the voltammograms showed that the peak potentials and corresponding currents varied at the different scan rates. This was an indication that the polymer is electroactive and the electron transfer processes were coupled to a charge transportation diffusion process, along the polymer. The first CGE/PANI/ABTS oxidation peak at 0.17V versus SCE indicated that the polyleucoemeraldine base (LB) converted to the polymeraldine salt (ES) at 0.45-0.5 V and ES to polypernigraniline salt (PS) at a potential of 0.57V vs SCE.

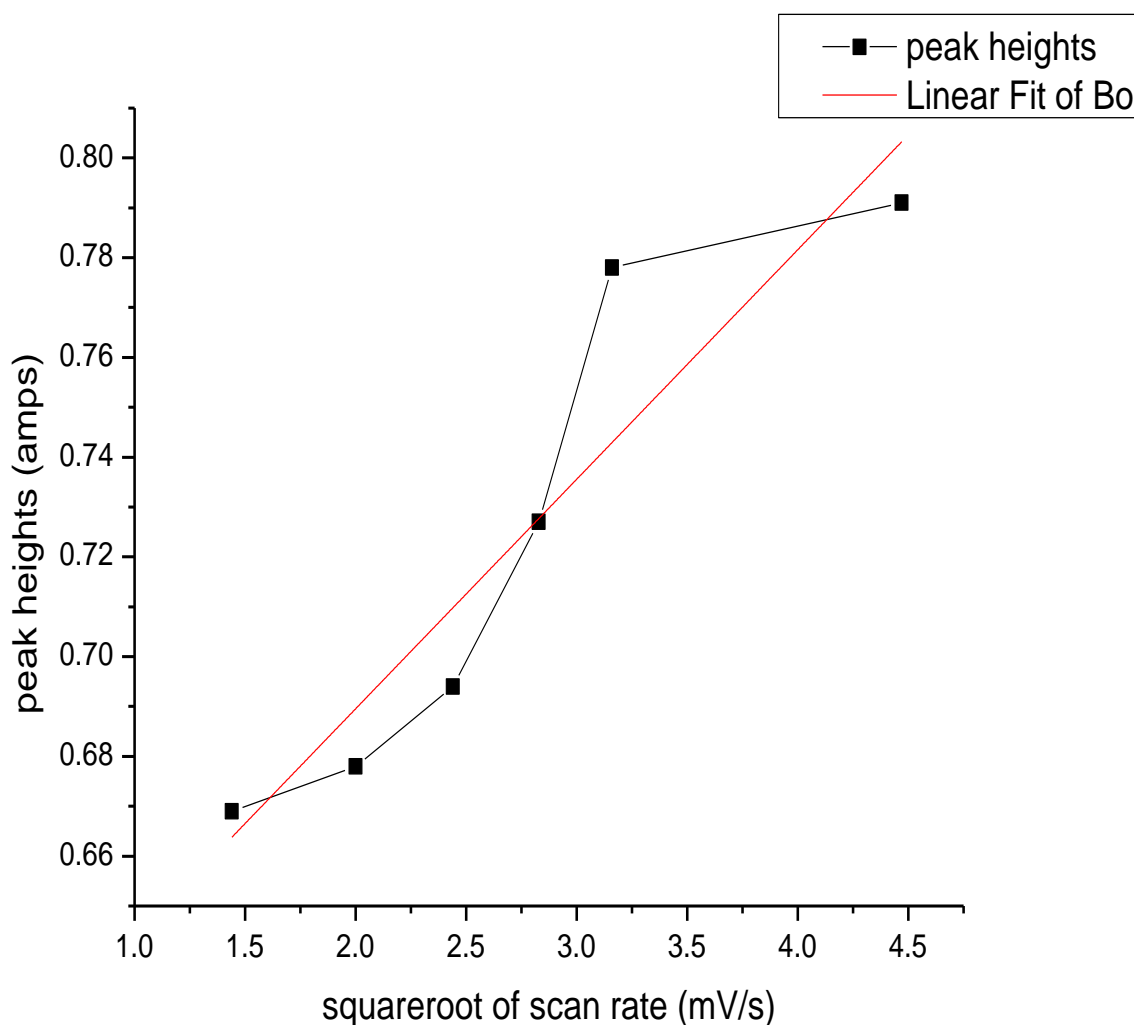


**Figure 7:** Randles Plot of peak currents versus square root of scan rate

The Randle plot that was obtained showed that the peak potentials and peak currents were increasing as the scan rate increased. The plot recorded an  $r^2$  value of 0.855 and a slope of 0.05 (red line which is line of best fit). Although this system is expected to be a diffusion controlled process, the low  $r^2$  value compared to unity could be indicative of slow electrode kinetics. In fact a transient behavior is seen in that there is adherence to linearity at very low scan rates. But as scan rate increases, the almost non-linear behavior manifested could mean inadequate time for the movement of flux to the electrode surface. Further, it could also be that the electron hopping process between the redox active polyleucoemeraldine peak (used for the plot) and the polyemeraldine salt (used for the plot) is slow and /or the adsorbed species are irreversibly transformed as indicated by the asymmetric voltammograms.

### 3.5. UV-Vis Spectrometry

The various films synthesized both electrochemically and chemically were subject to UV-Vis analysis to determine their spectroscopic behaviour. Figure 8 shows the UV-Vis spectrum of polyaniline prepared from a 0.1 M monomer concentration with 0.1 M HCl as supporting electrolyte in presence/or absence of ABTS. The peaks recorded were observed at wavelengths of 350nm as expected for protonic acid doped polyaniline [13]. The UV-Vis spectrum of the electrosynthesised PANi/ABTS was superimposed on the graph PANi/HCl plot. The presence of the polaronic peak at 446nm indicates that both HCl and ABTS are dopants.

Normally for a dedoped polyaniline system, the peaks at 350 nm are associated with the  $\pi$ - $\pi^*$  transition of the benzoid rings and a peak at around 650 nm is associated with the  $\pi$ - $\pi^*$  transition of the quinoid rings of the polyaniline backbone structure. This peak at 446nm observed in both PANi/HCl and PANi/ABTS is absent in either forms of the dedoped PANi. In the dedoped, disappearance of the polaronic peak at 446 nm gives way to the appearance of the quinonoid peaks at 650nm is indicative of a highly non- conductive polymer [18].

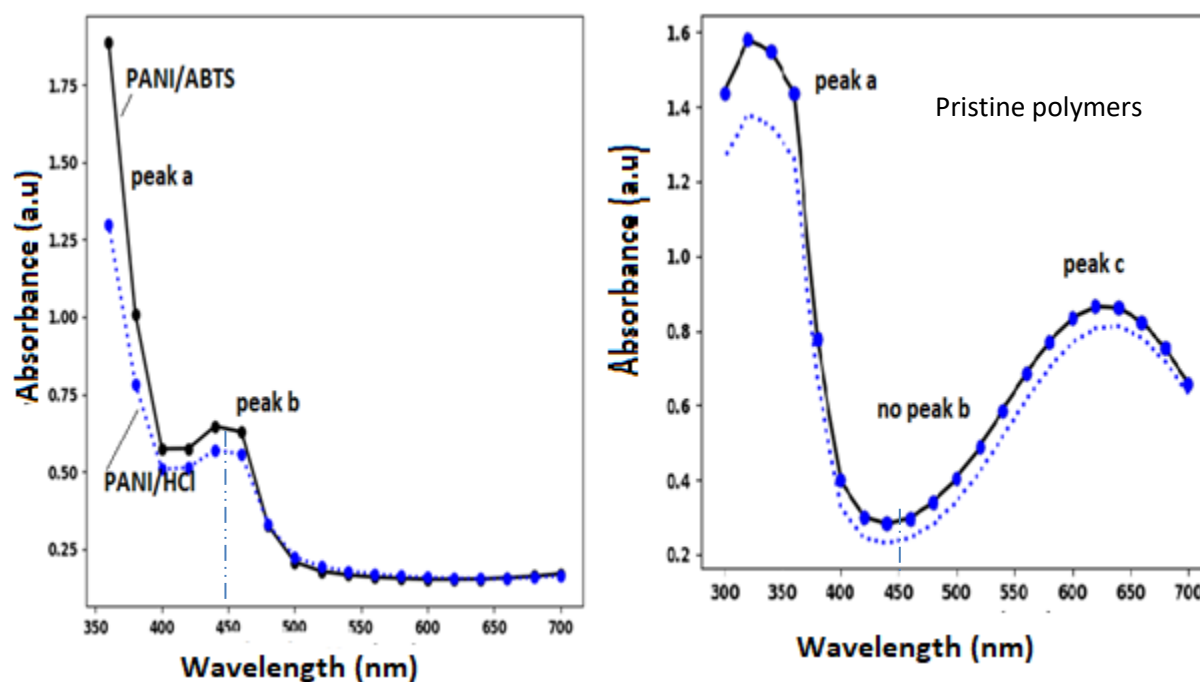


**Figure 8:** a) UV-Vis Spectrum of electrosynthesized polymer PANi/HCl and PANi /ABTS/in DMSO between 300 and 700nm in DMSO b) same films after dedoping in 0.2M NH<sub>4</sub>OH

Organic conducting polymers consist of a continuous valence and conduction band, separated by a band gap due to the overlapping of the p-orbitals. Due to the large size of the band gap in conducting polymers, intra-gap transitions are not energetically viable meaning that they are basically non-conductive. Interaction of these polymers in dopants, introduces new energy levels in the band gap, leading to them being converted to conductors or semi-conductors. Authors have associated the absorption round 450 nm in the polyaniline base UV-Vis spectrum to the incomplete /intermediate state formed during the oxidation of the polyeucoemeraldine salt of polyaniline and involves the three sub-band gap transitions [19]. It results from para- coupled phenyl -

structures corresponding to phenyl polarons [20]. The complete collapse of the quinonoid peak at 650 nm could be indication of complete doping and possible existence of bipolaron species an indication of improved conductivity [13].

### 3.6. The PANi/ABTS electrochemistry in Phosphate Buffer pH 7

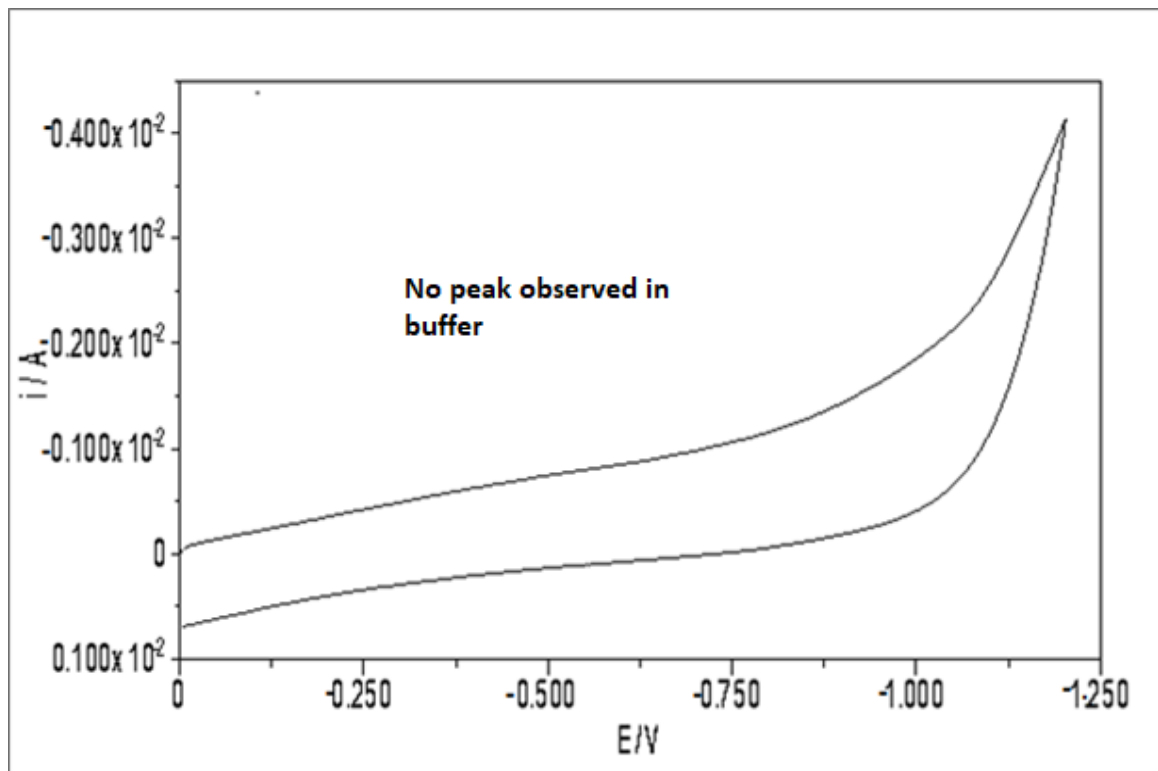


**Figure 9:** Cyclic voltammogram of PANi-ABTS on CGE electrode in 0.1M phosphate buffer (pH 7). No BPA analyte present

No peaks were observed in the PANi/ABTS/CGE electrode in 0.1M phosphate buffer indicating that the buffer is inert in the potential window 0 to -1.250 V used. Different electrochemistry was observed on introducing a small aliquot of hydrogen peroxide into this system.

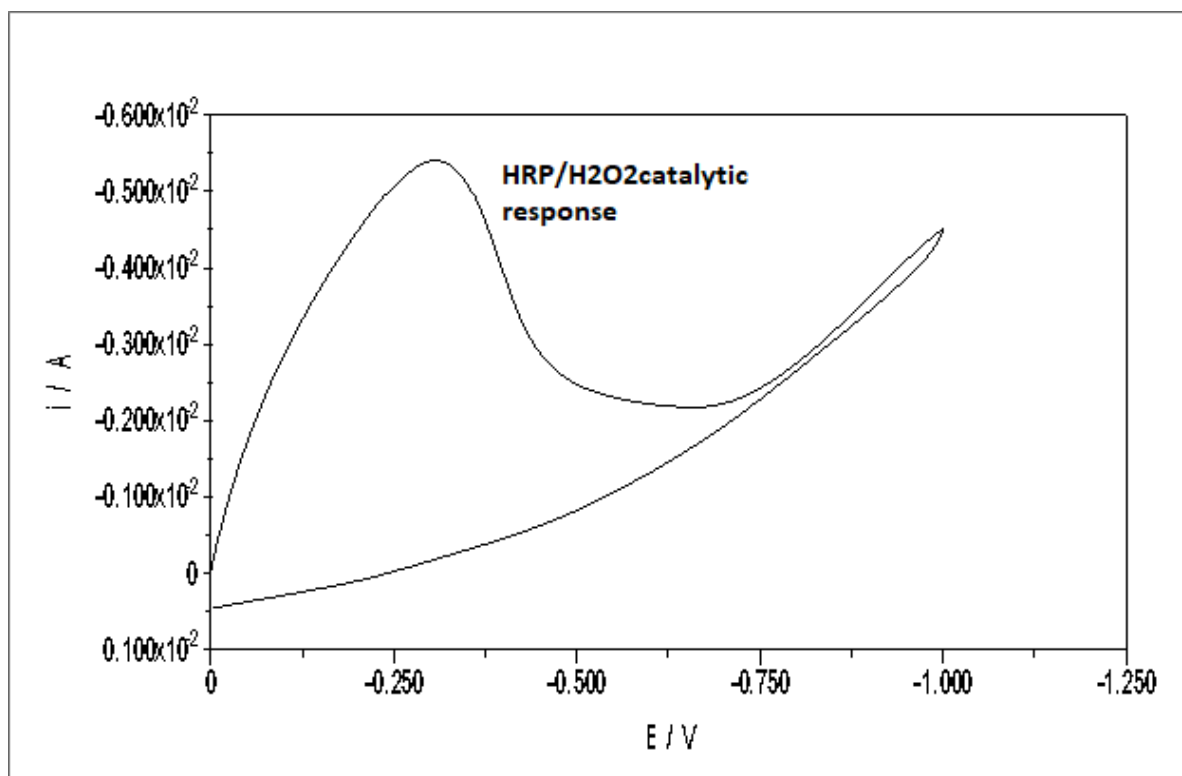


**Figure 10:** Cyclic voltammogram of PANi/ABTS/HRP on CGE electrode in 0.1M phosphate buffer pH 7 in the presence of  $8.8 \times 10^{-5}$  M  $\text{H}_2\text{O}_2$  (the HRP substrate). Figure shows a huge catalytic current due to enzyme substrate reaction

The HRP enzyme is generally a good substrate for hydrogen peroxide and gave a pronounced peak at around -0.250 V as seen in figure 10 above. The  $\text{H}_2\text{O}_2$  substrate receives two electrons from the CGE electrode via the PANi/ABTS system thus giving rise to the peak.

To this responsive HRP-hydrogen peroxide sensor system, bisphenol A was added and response monitored. On addition of a small aliquot of BPA to the above system, the catalytic peak observed when the HRP and  $\text{H}_2\text{O}_2$  interacts (Fig. 10 above) is de-attenuated. This means that there is electrochemical communication between the HRP enzyme and the BPA molecules- a phenomenon which forms the basis of sensor for BPA fabrication since the signal decrease can be related to the concentration of BPA present in solution.

It is deemed that BPA communicates electrochemically by giving electrons to the HRP and becomes oxidized resulting in the peak reduction due to inhibition (figure 11 below). A peak reduction by a magnitude of  $1.0 \times 10^{-2}$  (Fig 11 (a) and (b)) was realized. Seemingly both BPA and  $\text{H}_2\text{O}_2$  compete for the same HRP catalytic sites leading to signal de-attenuation (Fig. 11 (b)) below.

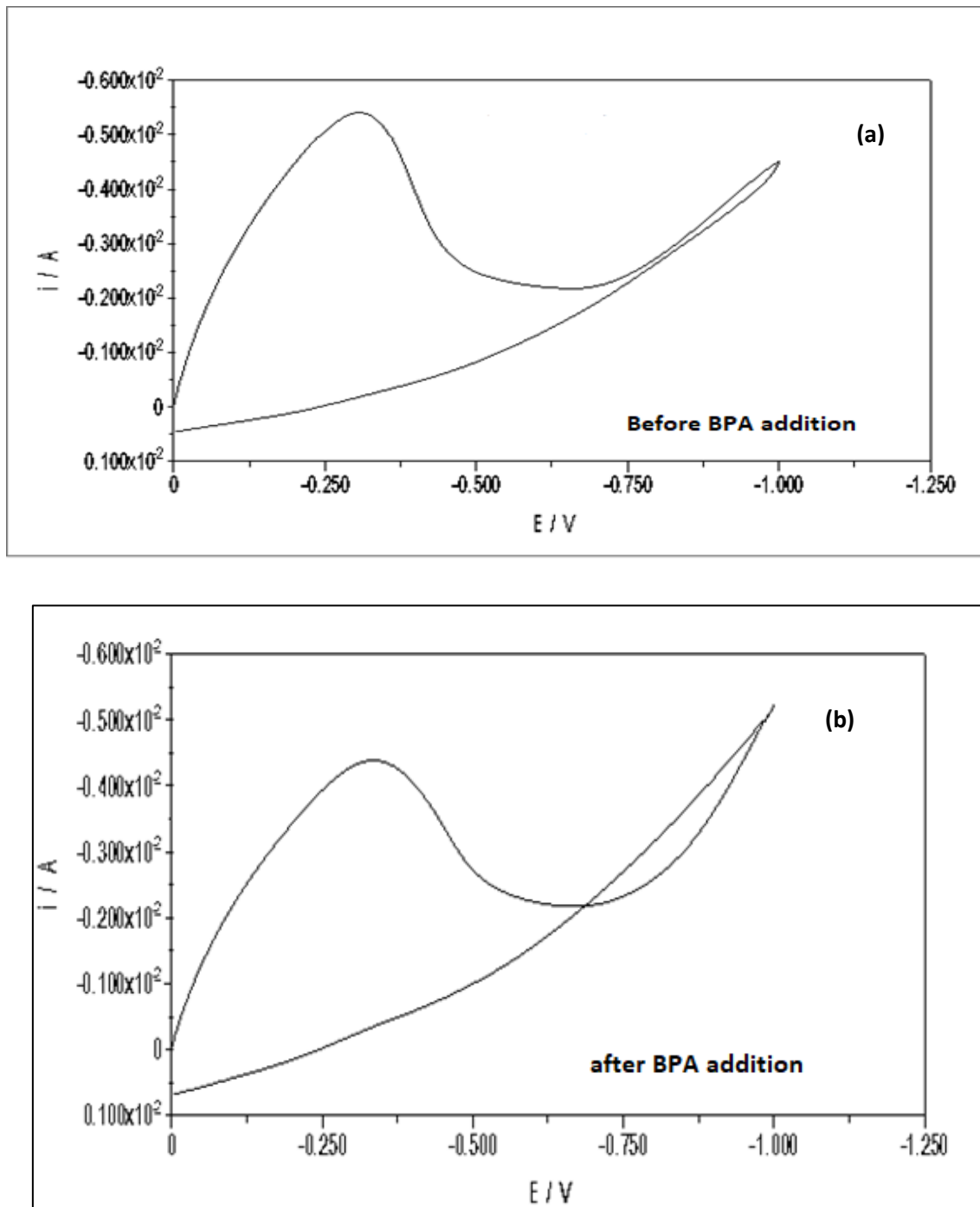


**Figure 11:** Cyclic voltamograms of a) CGE/PANi/ABTS electrode in 0.1M phosphate buffer pH 7 in presence of  $8.8 \times 10^{-5}$  M  $H_2O_2$  and no BPA and b) Same system as in a) but in the presence of BPA. Figure shows current response reduction in presence of BPA

### 3.7. CGE/PANI/ABTS/HRP Biosensor response to different concentrations of BPA

The CGE/PANI/ABTS/HRP biosensor for BPA was operated at a potential window of between 0 and -1.250 V at  $100\text{mVs}^{-1}$ . Initially the sensor was operated in the absence of BPA to obtain the maximum current response due to HRP interaction with hydrogen peroxide. The concentration of  $H_2O_2$  throughout all experiments was

maintained at 0.09 mM. The PANi-ABTS film was the electro-mediation medium shuttling electrons between the CGE electrode and the enzyme. Consequently small aliquots of BPA were added and the resultant currents monitored for decrease. The current signal decrease was correlated to the concentration of the BPA present in solution leading to the construction of the calibration curve. Peak de-attenuation occurred with increasing [BPA] and these preliminary results indicated the HRP-BPA interaction was inhibitive in nature. The peak currents responses for various BPA concentrations are recorded in Table 2 below.

**Table 2:** A table of concentration of BPA and peak heights

Concentration of BPA nM)	Peak Current (heights) $I_{pa}$ , (A) in presence of 0.09mM $H_2O_2$	Peak height difference due to conc. of [BPA]
0	$1.52 \times 10^{-4}$	0
125	$1.45 \times 10^{-4}$	$0.07 \times 10^{-4}$
625	$0.52 \times 10^{-4}$	$1.0 \times 10^{-4}$
1250	$0.042 \times 10^{-4}$	$1.48 \times 10^{-4}$
1875	$0.03 \times 10^{-4}$	$1.49 \times 10^{-4}$
2500	$0.009 \times 10^{-4}$	$1.51 \times 10^{-4}$

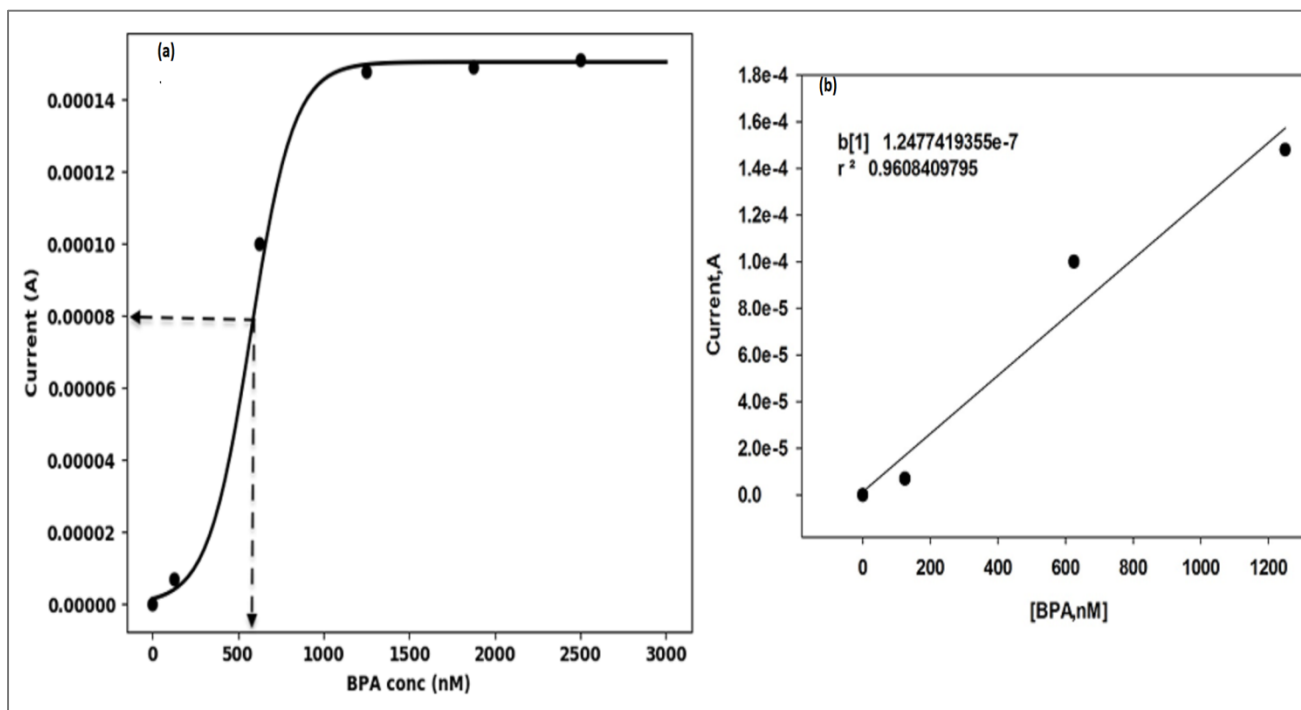


**Figure 12:** (a) Calibration curve for [BPA] between 0-2500nM, (b) The biosensor dynamic linear range.

The calibration curve recorded for the various concentrations of BPA between 0 and 2500nM is given in figure 12 above. The calibration curve shows a linear part where the current magnitude depends on the concentration of BPA. The levelling off of the calibration curve shows regions where substrate concentration has no effect on the enzyme because the enzyme active sites are already saturated. The linear part of the calibration curve is the one useful for the analytical purposes.

The dynamic linear range of the biosensor was determined to be between of 0 – 1200nM BPA (Fig. 12(b) above). This would be the effective linear range for analytical purposes and it could be deemed satisfactory, given the BPA concentrations that have been used. The sensitivity of the sensor was worked to be  $1.2477 \times 10^{-7}$  A/nM and compares well with those reported [21]. The apparent Michaelis Menten constant,  $K_m$  was also estimated to be 550 nM. This is shown as half the  $I_{max}$  on the linear part of the calibration curve. The biosensor seems to reach a quick saturation point due to easy inhibition of the enzymes active cites by BPA molecules. We recommend that more work could be carried out to optimize the biosensor operational parameters and to understand the nature of this inhibition.

### 3.8. Proposed HRP Catalytic Degradation Mechanism

The HRP catalytic degradation of hydrogen peroxide follows a ping-pong mechanism as shown in Figure 12 below [22]

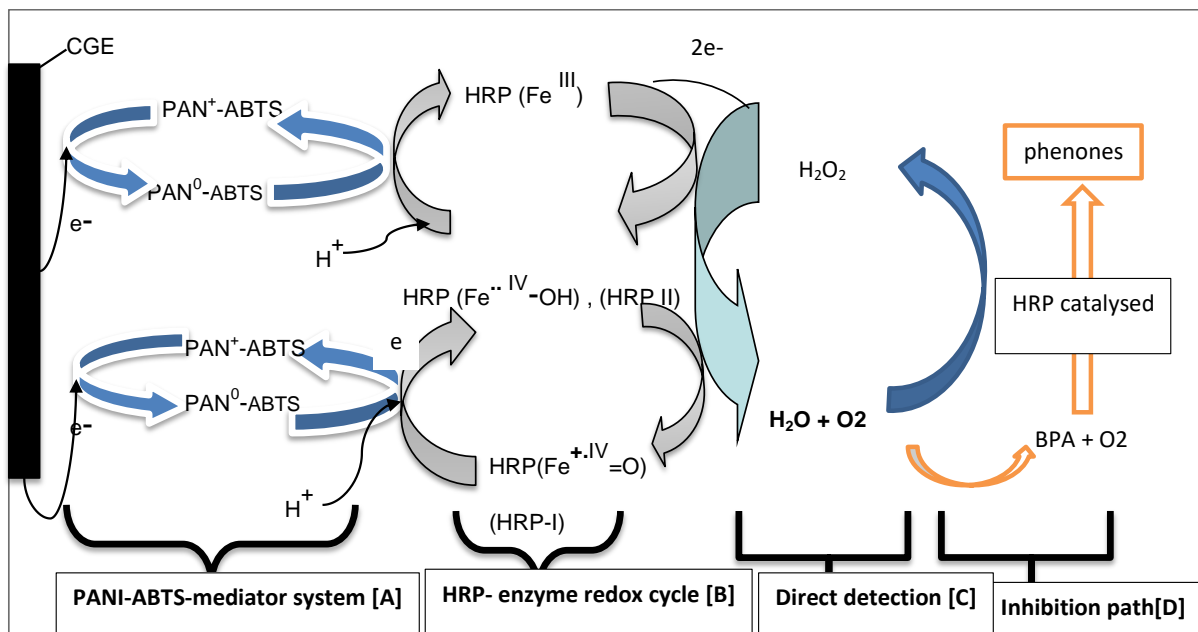


**Figure 12:** The HRP ping-pong mechanism showing the reduction of H<sub>2</sub>O<sub>2</sub> and oxidation of BPA to various products

The mechanism involves the enzyme undergoing a certain redox cycle in which in the presence of a suitable electron shuttler. In the reduction of hydrogen peroxide in the body, the electron shuttler/mediator is NADP. It then undergoes a series of reduction and oxidation steps. In the process the enzyme is able to catalyse the oxidation or reduction of certain substrates. In our ex-situ situation, the PANI/ABTS system is the electron shuttler/mediator.

The detection of BPA occurs via an inhibition process involving the HRP enzyme. Firstly, the HRP in the resting state accepts two electrons from the electrode (by lowering its Fermi level) via the PANI/ABTS mediator. HRP enzyme in its resting state is characterized by a ferric redox center which can alternatively undergo oxidation enabling it to switches between the oxidized and reduced forms.

Steps involved in the detection of HRP and consequently BPA involve;

I) The acceptance of electrons by the polyaniline/ABTS mediator-system from the electrode. In this case the polyaniline polymer is reduced from the oxidized form (PAN<sup>+</sup>-ABTS) to reduced form ( PAN<sup>0</sup>-ABTS), ( represented by part [A] in the scheme above).

1) The reduced form of PANi-ABTS next passes the electron to the HRP-Fe<sup>3+</sup> (in its resting state) and thus the enzyme becomes reduced to the hydroxyferryl state HRP- (Fe<sup>IV</sup>-OH) also known as the HRP-II state [23]. A second electron passed to the enzyme in its HRP-II state by a second PANi-ABTS molecule reduces the enzyme to the oxyferryl state HRP-(Fe<sup>IV</sup>=O) [22, 23] also known as HRP-I state which is two reducing equivalents below its resting state. One equivalent being on the prosthetic group and the other being on the porphyrin ring [23] (Part B of the Figure 12)

2) To bounce back to its resting state, the HRP enzyme in a series of two steps donates two electrons to the hydrogen peroxide substrate In the process, the enzyme loses two electrons to the hydrogen peroxide substrate in solution which as per the following reaction.

Meanwhile, the substrate H<sub>2</sub>O<sub>2</sub> is converted to water and oxygen which can combine to oxygen (Part C of the Figure 12)



3) Finally the oxygen formed then oxidizes the BPA in solution in the presence of HRP enzyme to produce phenones [24] (Part D of the Scheme)

The fact that both the reduction of H<sub>2</sub>O<sub>2</sub> and oxidation of BPA is catalysed by the same enzyme means that there is a possibility of competition for the active sites [D]. It is thought that BPA forms strong interactions with the enzyme thus blocking some of the active sites leading to signal decrease. Thus as revealed in the sensor, addition of BPA led to a fall on the amperometric signal. The magnitude of decrease was observed to be proportional to the concentration of the BPA inhibitor in solution. The above cycle then repeats itself [22,23].

#### **4. Conclusion**

The detection of BPA on a graphite carbon/ polyaniline-2, 2'-Azinobis (3-ethylbenzothiazoline-6-sulfonic acid)/Horse radish peroxidase (GCE/PANI/ABTS/HRP) electrode was presented. Results showed that the presence of the ABTs surfactant in PANI gave rise to better electrochemistry compared to those of PANI/HCl, the former demonstrating near Nernstian behaviour especially in the middle peaks. Three redox pairs were observed in the PANI-ABTS system as compared to two in the PANI/HCl system. The presence of polaronic bands at 446nm, the diminished band at around 650nm due to pi - transitions of the quinonoid structures indicated the PANI/ABTS and PANI/HCl structures were conductive. The doping was mainly protonic as exposure of the composites to Ammonia solution removed the polaronic bands. While as there was no redox peak observed in the GCE/PANI/ABTS/HRP electrode in phosphate buffer solution in the absence of hydrogen peroxide, a huge peak at -0.250mV was observed on adding  $8.8 \times 10^{-5}$  M  $H_2O_2$ ; It was observed that addition of different concentrations of BPA in the presence of a known  $H_2O_2$  concentration lead to a HRP/ $H_2O_2$  amperometric signal de-attenuation. This indicated a possible catalysation of BPA oxidation by the same enzyme via inhibition. The HRP/BPA inhibition sensor gave a dynamic linear range of 0-1200nm with a sensitivity of  $1.2477 \times 10^{-7}$  A/nm and an apparent Michaelis Menten Kinetics of 550nm.

#### **5. Data Availability**

This work presents MSc. Work under examination. Data is available upon consultation.

#### **6. Limitations of the study**

This study was based on a relatively small sample size due to unavailability of resources. The cyclic voltammograms were taken on an inverted potentiostat which was difficult to obtain flexible graphs as with modern potentiostats

#### **7. Conflict of Interest**

There is no conflict of interest as far as we are concerned

#### **8. Funding Statement**

Authors would like to acknowledge Nacosti Kenya for Funding

#### **Acknowledgements**

Authors would like to thank the physics Department, university of Nairobi for availing their Bioanalytical Systems Electrochemical Workstation for the work

## References

- [1] Bolden, J. R. (2015). Bisphenol S and F: A Systematic Review and Comparison of the Hormonal Activity of Bisphenol A Substitutes. *Environmental Health Perspectives*, 643–650
- [2] Jone Corrales, L. A. (2015). Global Assessment of Bisphenol A in the Environment: Review and Analysis of Its Occurrence and Bioaccumulation. *SAGE journals*, 1-29
- [3] Beal, J. A. (2018). Baby Bottles and Bisphenol A (BPA). *The American Journal of Maternal/Child Nursing*, 349
- [4] Silva, M. S. (2012). Chemical Engineering Science. *Science Direct*, 94-100
- [5] Scientific Opinion on the Risks to Public Health related to the presence of Bisphenol A (BPA) in foodstuffs; Executive summary, EFSA journal, 2015, 13(1) 3978
- [6] Paseiro-Lopez, J. L.-C. (2010). Determination of bisphenol A in, and its migration from, PVC stretch film used for food packaging. *Food Additives and Contaminants*, 596-606.
- [7] Jones, B. A. (2012). Perinatal Bisphenol A administration alters. *SIMON FRASER UNIVERSITY*
- [8] Yoon Jung Yang, Y.-C. H. (2009). Bisphenol A exposure is associated with oxidative stress and inflammation in postmenopausal women. *ELSEVIER- Environmental Research*, 797-801
- [9] Vanage, D. T. (2017). Bisphenol A Induces Oxidative Stress in Bone Marrow Cells, Lymphocytes, and Reproductive Organs of Holtzman Rats. *SAGE- International Journal of Toxicology*, 35-98
- [10] Ganesh, A. M. (2014, July 02). Horseradish Peroxidase Enzyme Immobilized Graphene Quantum Dots as Electrochemical Biosensors. *Applied biochemistry and biotechnology*, pp. 945-959
- [11] Nkunu Z. N., Kamau G.N., Kithure J.G., Muya C.N, Electrochemical studies of potassium ferricyanide in acetonitrile-water media (1:1) using cyclic voltammetric method, *International journal of scientific research and Innovative technology*, vol 4, issue 5, 2017, 52-56
- [12] Monk P. M. S., (2001). *Fundamentals of electroanalytical chemistry*. Wiley & Sons, NY, USA, pp 17-24
- [13] MacDiarmid A. G. (2001). "Synthetic Metals": A Novel Role of Organic Polymers (Nobel Lecture)\*\*. *Angewandte Chemie International Edition*, 40: 2581-2590
- [14] Lindfors T., and Ivaska A. (2002). pH sensitivity of polyaniline and its substituted derivatives. *Journal of electroanalytical Chemistry*, 531: 43-52

- [15] Hino T., Namiki T., Kuramoto N. (2006). Synthesis and characterization of novel conducting composites of polyaniline prepared in the presence of sodium dodecyl sulfate and several water soluble polymers. *Synthetic Metals*, 156: 1327-1332
- [16] Ramamurthy V, Gomathi H., Kan J. K., (2006). Beneficial reole of surfactants in electrochemistry and in the modification of electrodes. *Advances in colloid and interface science*, 119(1) 22-68
- [17] Mahnaz Abdi, Paridah Tahir, ramaida Liyana, Ramin Javahershenas, A surfactant directed Microcrystalline cellulose/polyaniline composite with enhanced electrochemical properties, *Molecules*, 2018, 23(10) 2470
- [18] Kim J., Kwon S., Ihm D. (2007). Synthesis and characterization of organic soluble polyaniline prepared by one step emulsion polymerization. *Current Applied Physics*, 7:205-210
- [19] Bernard M. C., Goff A.H., Joiret S., Arkout H., saïdani B. (2005). Influence of the nature of substituents on charge mechanisms in substituted polyanilines (SPANi, POMA) studied by Raman and optical spectroscopies. *Electrochimica Acta*, 50:1615
- [20] Malinauskas A., Malinauskienė J., Ramnavičius A. (2005). Conducting polymer-based nanostructured materials: Electrochemical Aspects. *Nanotechnology*, 16: R51-R62
- [21] Mitsuru Yohshida, Hiroshi Ono, Yoshiko Mori, Yoshihiro Chuda, Koichi Onishi, Oxidation of Bisphenol A and related compounds. (2001). *Journal of Bioscience Biotechnology Biochemistry*, 65 (6) 1444-1446
- [22] Panzarasa G., The horseradish smile: demonstrating chractersitic reactions of peroxidases in a visually appealing way. (2020). *Biochemistry and Molecular Biology Education*, vpl48, issue 1, 38-43
- [23] Iwuoha E. I., Saenz de Villaverde D., Garcia N. P., Smyth M. R., Pingarron J. M. (1997). Reactivities of organic phase biosensors. 2. The amperometric Behaviour of horseradish peroxidase immobilised on a platinum electrode modified with an electrosynthetic polyaniline film. *Biosensor and Bioelectronics*, 12: 749-761
- [24] C.Emmelmanna, P. M. (2011). Laser Additive Manufacturing of Modified Implant Surfaces with Osseointegrative Characteristics. *ELSEVIER - Physics Procedia*, 375-384.
- [25] Zhuo Ye, Q. W. (2019). Simultaneous detection of bisphenol A and bisphenol S with high sensitivity based on a new electrochemical sensor. *Journal of Electroanalytical Chemistry*, 676